Identification of the Cavitation Flow Parameters on the Basis of Photofixing of an Experimental Supercavity

[1]Vladimir Serebryakov*

[1]*Institute of Hydromechanics of the National Academy of Sciences, Ukraine*

Abstract

The method of accelerated estimation of supercavitating flow key parameters is proposed for the experimental study of nearly axisymmetric flows. The refinement of the elemental equations controlling the cavity shape with the account of gravity and cavitator lift effects is presented.

Keywords: supercavitation; theoretical and experimental substantiation; axisymmetric flow.

Introduction

Numerous experimental study of nearly axisymmetric supercavitating flows proved a practical independence of the expansion cavity sections in immobile fluid from each other. The effect of free boundary and rigid walls at not too small depth on the cavity shape only slightly changes the initial shape observed in the infinite flow, although the flow boundaries can strongly affect the cavity size and elongation. Moreover, even in case of strong perturbations of the cavity shape within its certain portion, e.g., where a body is planing along the cavity surface, the adjoining cavity surface portion behind the planing zone exhibits very small variations. The intrinsic features of nearly axisymmetric supercavitating flows make it possible to elaborate a procedure for the estimation of the cavitating flow key parameters, including cavitation and Froude numbers, as well as the cavity shape, which would correspond to the infinite flow conditions, by matching some unperturbed part of the cavity observed under test conditions with a quite accurate equation controlling the cavity shape in the infinite flow.

Asymptotic models describing the nearly axisymmetric cavity shape and dimensions

The integro-differential equation (IDE) controlling the shape of a stationary axisymmetric cavity in subsonic flow, which has been derived via the Hydrodynamics of Slender Body approach for the small cavitator model is used as the initial basic equation in the developed technique:

$$\frac{1}{2R^2}\left(\frac{dR^2}{dx}\right)^2 + \frac{d^2R^2}{dx^2}\ln\frac{\beta^2R^2}{4x(L-x)} - \int_0^L \frac{\frac{d^2R^2}{dx^2}\Big|_{x=x_1} - \frac{d^2R^2}{dx^2}}{|x_1-x|}dx_1 - \frac{\frac{dR^2}{dx}\Big|_{x=0}}{x} + \frac{\frac{dR^2}{dx}\Big|_{x=L}}{L-x} = 2\sigma(x), \qquad (1)$$

where r, x are polar co-ordinates at $x=0$ in the flow separation section, $r=R(x)$ is the cavity shape, $\sigma = 2\Delta P/\rho U_\infty^2$ is the cavitation number, $\Delta P = (P_\infty - P_c)$ is the difference of pressures in the flow P_∞ and cavity P_c, U_∞ is velocity of the incident flow, ρ is fluid mass density, parameter $\beta = \sqrt{1-M}$, where M is the Mach number. The reduction of cavitation numbers to $\sigma \to 0$ leads to the unlimited increase in the cavity dimensions and elongation $\lambda \to \infty$, making the cavitator size negligible with the order of magnitude of O[$(1/\lambda^2)\ln\lambda$], in comparison with the cavity length. The problem analysis within the framework of MAEM (matched asymptotic expansion method) implies the structure of the singular solution for the cavity shape $R = R(x,\lambda)$ at $1/\lambda \to 0$. This structure includes: (i) an interior non-linear solution for a disk within a small area O[$(1/\lambda^2)\sqrt{\ln\lambda}$] in the cavitator vicinity, (ii) an intermediate solution for the cavity front part having the well-known asymptotic form for flow expansions in the infinity, which is refined by adding the third term (2a), and (iii) an exterior solution in the form of ellipsoid perturbation (2b).

$$\text{a) } R^2 = \frac{2\sqrt{c_{do}}\,x}{\sqrt{\ln x}}\left[1 - \frac{1}{4}\frac{\ln\ln x}{\ln x} + \frac{1}{2}\frac{\ln\left(e\sqrt{c_{do}}\beta^2/2\right)}{\ln x}\right], \quad \text{b) } R^2 = \frac{1}{\lambda^2}\left[(1-x^2) + \frac{x^2\ln 4 - \ln(1+x)^{(1+x)} - \ln(1-x)^{(1-x)}}{\ln(\lambda/\beta)^2}\right], \qquad (2)$$

The exterior solution (2a) is derived in the form of two terms of the asymptotic series at $1/\lambda \to 0$. Noteworthy is that the dimensions of zones corresponding to interior and intermediate solutions, including the cavitator size, are neglected with an order of magnitude $O(1/\lambda^2)$. In solution of (2b), $x=0$ corresponds to the cavity midsection with

*Corresponding Author, Vladimir Serebryakov: serebryakov_vladimir@yahoo.com

its normalization by the cavity semi-length L_k. The second-order dependence $\sigma = \sigma(\lambda)$ (3a) is also derived, while the inverse relationship $\lambda = \lambda(\sigma)$ is calculated via successive approximations of equations (3b-3c)

$$\text{a)}\ \sigma = \frac{\ln(\lambda/\beta)^2}{\lambda^2}\left[1 - \frac{1}{\ln(\lambda/\beta)^2}\right],\ \text{b)}\ \sigma = \frac{2\mu}{\lambda^2} \to \text{c)}\ \mu = \frac{1}{2}\ln\left(\frac{2\mu}{e\beta^2\sigma}\right);\ \text{d)}\ R_k^2 = R_n^2\frac{c_d}{\sigma}\left[1 + 2\frac{\ln 2/\sqrt{e}}{\ln(\lambda/\beta)^2}\right], \quad (3)$$

Matching of intermediate (2a) and exterior (2b) solutions yields the dependence controlling the cavity maximal radius R_k (3d), where $c_d|_{\sigma=0} = c_{do}$ is the cavitator drag coefficient. In view of a slow variation of parameters μ and k in decompositions (3a-3d), the dependences controlling the cavity basic dimensions in the form of (4a-4c) are:

$$\text{a)}\ \lambda^2 = \frac{2\mu}{\sigma}; \qquad \text{b)}\ R_k^2 = R_n^2\frac{c_d}{k\sigma}; \qquad \text{c)}\ L_k = \frac{R_n}{\sigma}\sqrt{\frac{2c_d\,\mu}{k}},$$

$$\text{d)}\ \mu \approx \ln\sqrt{\frac{1}{e}\left(\frac{\lambda^2}{\beta^2}+7\right)},\ \mu \approx \ln\sqrt{\frac{1}{e\beta^2\sigma}\ln\left(\frac{2}{\beta^2\sigma}+10\right)};\quad \text{e)}\ k \approx 1 - \frac{2\ln\left(2/\sqrt{e}\right)}{\ln\left(0.8(\lambda/\beta)^2+35\right)},\ k \approx 1 - \frac{2\ln\left(2/\sqrt{e}\right)}{\ln\left(4/\sigma^2+18\right)} \quad (4)$$

Based on the non-linear numerical simulation results [1], the dependences for μ and k were refined to the form of (4d-4e) for the case of streamlined flow past cones, including a disk, with maintenance of their asymptotic structure. This refinement improves the accuracy of equations for the cavity basic dimensions (4b-4e) within the range of cavitation numbers $\sigma = 0 \div 0.2$ to the level achieved within the framework of the second-order non-linear theory.
For small values of the inverse elongation parameter $1/\lambda_*$ of the "axisymmetric cavitator – cavity" system, IDE (1) in the limiting case of $1/\lambda_* \to 0$ is reduced to a differential equation. The latter is refined by coefficients μ and k, while the MAEM matching operation is replaced by introducing the conservation equation of energy transferred from the cavitator to the cavity during its motion in a fluid, which allows one to develop a quite effective approach for calculation of the supercavity flows [4]. Taking into account a small-scale variation of parameters μ and k, it becomes applicable for calculation of various cases of stationary and nonstationary flows. The cavity shape $R = R(x)$ for stationary streamlined flows is controlled by the set of equations (5) with the normalization of x and R by the cavitator radius R_n, which may be classified into two variants: A and B.

Variant **A**

$$\text{a)}\ \frac{d^2R^2}{dx^2} + \frac{\sigma(x)}{\mu_c} = 0,\ \text{b)}\ \frac{\mu_c}{\mu} = \left(\frac{2}{\sqrt{1-k\sigma/c_d}+1}\right)^2,$$

$$\text{c)}\ \left.\frac{dR^2}{dx}\right|_{x=0} = \sqrt{\frac{2(c_d - k\sigma)}{k\mu_c}},\quad \left.R^2\right|_{x=0} = 1,$$

Variant **B**

$$\text{d)}\ \frac{d^2R^2}{dx^2} + \frac{\sigma(x)}{\mu_m} = 0,\ \text{e)}\ \frac{\mu_m}{\mu_c} = \left(1 - \frac{x_*}{L_m}\right)\left(\frac{1 - \dfrac{k\sigma}{c_d}}{1 - R_*^2\dfrac{k\sigma}{c_d}}\right),$$

$$\text{f)}\ \left.\frac{dR^2}{dx}\right|_{x=x_*} = \sqrt{\frac{2(c_d - k\sigma R_*^2)}{k\mu_m}},\quad \left.R^2\right|_{x=x_*} = R_*^2,$$

$$\text{g)}\ x_* \geq e:\quad R_*^2 = 2x_*\left.\sqrt{c_{do}/\ln x}\right|_{x=e} = 2e\sqrt{c_{do}} \quad (5)$$

$$\text{a)}\ R^2 = 1 + \sqrt{\frac{2(c_d - k\sigma)}{k\mu_c}}x - \frac{\sigma}{2\mu_m}x^2,\qquad \text{b)}\ R^2 = R_*^2 + \sqrt{\frac{2(c_d - k\sigma R_*^2)}{k\mu_m}}(x - x_*) - \frac{\sigma}{2\mu_m}(x - x_*)^2, \quad (6)$$

$$\text{a)}\ R_k = \sqrt{\frac{c_d}{k\sigma}}\ \text{b)}\ L_m = \frac{1}{\sigma}\sqrt{\frac{2\mu_c(c_d - k\sigma)}{k}},\quad \text{c)}\ L_k = \frac{1}{\sigma}\sqrt{\frac{2\mu_c c_d}{k}},\quad \text{d)}\ L_c = \frac{R_n}{\sigma}\sqrt{\frac{2\mu_c}{k}}\left(\sqrt{c_d - k\sigma} + \sqrt{c_d}\right) \quad (7)$$

The variant **A** with equations (5a-5c yields the solution (6a) for $\sigma = \text{const}$, which corresponds to an ellipsoidal cavity and provides a sufficient cavity shape prediction accuracy, including its maximal sizes by equations (7): radius R_k, for the cavity portion between its front part and midsection L_m and even for a limited length behind the midsection L_k/ However, it fails to predict the cavity shape in the vicinity of a disk-type cavitator. A slight refinement of parameter μ in the form of Eq. (5b) for μ_c precise cavity sizes to more realistic prediction for the cavitator vicinity zone. An essential refinement of the cavity shape prediction for its medial part (Figure 1), is reached by the application of the set of equations (5d-5g) of variant **B**. This makes it possible to predict the cavity shape starting from section $x \geq x_*$ where the first term of asymptotic dependence (5g) quite accurately controls the cavity shape. The adjustment of parameter μ_c in the form of Eq. (5e) for μ_m (5e) allows one to assess cavity dimensions via Eq. (7).

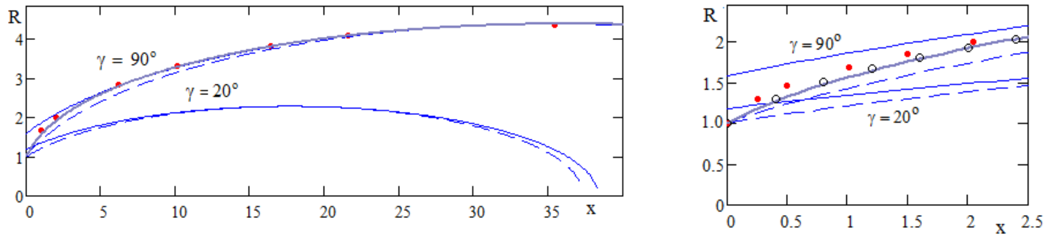

Figure 1. Shape calculation results at $\sigma = 0.05$ for a cavity behind a disk and a cone at $\gamma = 20^o$:

---- - Eq. (6a), ———— Eq (6b), ▬▬▬ - Eq (8), • • • • - numerical simulation [1], ∘ ∘ ∘ ∘ - experiment [2]

More exact calculation of the axisymmetrical cavity shape can be performed via set of equations (9), where Eq.(9a) was derived by adding a symmetrical part to the operator of Eq.(8), which controls the asymptotic dependence (2a). Further this operator is transformed into operator (9a), converting pressure values at the paraboloid, which approximates the cavity front part, into accurate values, allowing one to refine the solution for the cavity front part shape. Finally equation (9a) approximates IDE (1) via the energy conservation equation with an approximate account of energy transfer in the axial direction with help of coefficient k.

$$\frac{1}{2R^2}\left(\frac{dR^2}{dx}\right)^2 + \frac{d^2R^2}{dx^2}\ln\frac{\beta^2R^2}{4x^2} - \frac{1}{x}\frac{dR^2}{dx} = 0 \tag{8}$$

$$\text{a)}\ \frac{1}{2\left(R^2+R_f^2\right)}\left(\frac{dR^2}{dx}\right)^2 + \frac{d^2R^2}{dx^2}\ln\left[\frac{4(x+\Delta)^2(L+\Delta-x)^2}{\beta^2\left(R^2+R_f^2\right)L}\right] - \frac{dR^2}{dx}\left[\frac{1}{x+\Delta} - \frac{1}{L+\Delta-x}\right] = 2\sigma,$$

$$\text{b)}\ \left.\frac{dR^2}{dx}\right|_{x=0} = \sqrt{\frac{2(c_d-k\sigma)}{k\ln\left[2\Delta(1+\Delta/L)/\beta\sqrt{1+R_f^2}\right]}}\ ,\quad \left.R^2\right|_{x=0} = R_n^2;\quad \text{c)}\ R_f = \sqrt{\frac{c_d}{\ln x_*} - \frac{\kappa_r}{2x_*}},\ \text{d)}\ \Delta = \frac{1}{2}\left(\frac{1}{R_f} + R_f\right), \tag{9}$$

Here R_f is curvature radius of the paraboloid approximating the cavitator generatrix at $\kappa_r = 1$. The calculation results obtained via (9) for the medial and front part of a cavity are depicted in Fig.1.
Dependences for the cavity axial distortion induced by the effects of gravity h_g and cavitator's angle of attack α are represented by the set of equations (10a), governing dependence [2] and the solution in quadratures (10b):

$$\text{a)}\ \frac{d}{dx}\left(R^2\frac{dh}{dx}\right) - \frac{gR^2}{U_\infty^2} = 0\quad \left.\frac{dh}{dx}\right|_{x=0} = h'_{xo}\quad h|_{x=x_o} = h_o:\ \text{b)}\ h = \frac{g}{U_\infty^2}\int_{x_o}^{x}\frac{1}{R^2}\int_{x_o}^{x}R^2dx + h'_{xo}\int_{x_o}^{x}\frac{R_o^2}{R^2}dx + h_o,\ h'_{xa} \approx \tan\alpha \tag{10}$$

$$\text{a)}\ \frac{h_g}{R_n} = \left(\frac{L_k}{R_n}\right)^2\left(\frac{gR_n}{U_\infty^2}\right)\frac{2}{3}\left\{\ln\frac{2-\bar{a}}{(2-\bar{a})-\bar{x}} + \frac{1}{4}\left[\bar{x}^2 - 2\bar{x}(1-\bar{a})\right] - \frac{\bar{a}^2}{4}\left(1-\frac{\bar{a}}{3}\right)\ln\frac{(2-\bar{a})(\bar{a}+\bar{x})}{\bar{a}[(2-\bar{a})-\bar{x}]}\right\},\quad \bar{x} = \frac{x}{L_k},\ \text{b)}\ \bar{a} = 1 - \sqrt{1-\frac{k\sigma}{c_d}},$$

$$\text{c)}\ \frac{h_g}{R_n} \approx \left(\frac{L_k}{R_n}\right)^2\frac{gR_n}{U_\infty^2}\left(\frac{(\bar{x}+\bar{a})^{2.2} - \bar{a}^{2.2}}{3.2}\right),\quad \text{d)}\ \frac{h_\alpha}{R_n} = \frac{c_{dy}}{2}\frac{L_k}{R_n}\frac{k\sigma}{c_d}\ln\frac{(2-\bar{a})(\bar{x}+\bar{a})}{\bar{a}[(2-\bar{a})-\bar{x}]},\quad \text{e)}\ h_{g\alpha} = h_g + h_\alpha, \tag{11}$$

The dependence for the cavity shape $R = R(x)$ in the integral form of (10b) is the most accurately controlled by set of equations (9). In analytical solutions (11), for the flow separation section $x = 0$, dependence (6a) is used. The solution for h_α (11d) holds for the range of cone opening semi-angles $\gamma < 25^o \div 35^o$. For blunter cone- or disk-type cavitators, it is required to use a more accurate dependence $R = R(x)$ to in integral (10) for cavity sections $x < x_*$.

Identification of cavitation number via the experimental cavity profile photos

Given a feeble effect of some perturbations on the cavity shape under test conditions, except for the essential variation of its dimensions, it is expedient to use the adjusted cavitation number σ_a, which controls the cavity shape in the infinite flow. It may differ from that calculated via the test pressure value in cavity P_c as $\sigma = 2(P_\infty - P_c)/\rho U_\infty^2$. Estimate of σ_a can be made by the numerical solution of Eq.(12) using the experimental cavity radius R_a measured at an arbitrary section $x = X_a$. The cavity shape in Eq. (12b) is taken from Eq (6b):

$$\text{a) } \Delta\sigma(x) = -2\frac{gRn}{U_\infty^2}\int_0^x\int_0^x h_{g\alpha}dxdx \text{ , b) } \sigma = \frac{2\mu_m}{(X_a - x_*)^2}\left[\sqrt{\frac{2(c_d - k\sigma R_*^2)}{k\mu_m}}(X_a - x_*) - \left(R_a^2 - R_*^2\right) + \frac{2}{\mu_m}\left(\frac{gR_n}{U_\infty^2}\int_0^{x_a}\int_0^{x_a} h_{g\alpha}dxdx\right)\right] \quad (12)$$

The actual and calculated shapes of an artificial cavity formed behind a cone of 50mm-diameter with opening semi-angle of 20^o in a zero angle α_n of attack for motion at depth of 150mm are compared in Figure 2.

a)

b)

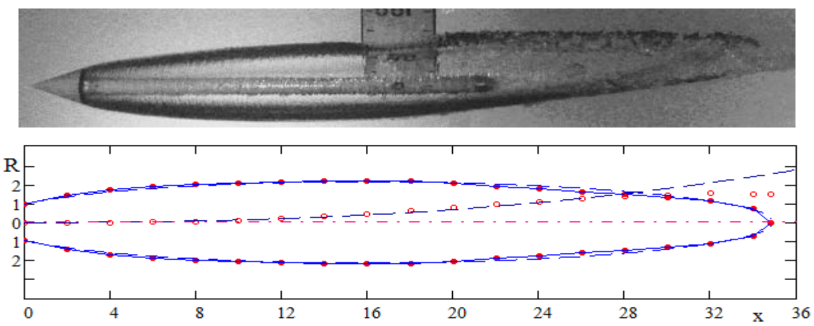

Figure 2. Photo experimental cavity behind a cone with a zero attack angle with calculated cavity contour – Eq (6a), accounting Eq. (12a) and axial distortion of it's axis – Eq.(11c)

$U_\infty = 7.12 m/s$, $Q_v \approx 0.00134 m^3/s$, $\alpha_n = 0$, $Fr \approx 14.38$: ─•─•─ Experimental data, – – – – – calculation $\sigma_a = 0.056$, Eq (12)

The adjusted cavitation number $\sigma_a \sim 0.056$ calculated via Eq. (12) used Eq. (6b) from the cavity radius measured at sections $X_a = 10$ differ from that derived in [5] with an account of free boundary effect only by ~5-6 %. However, the proposed method application requires and accurate and reliable measurement of the cavity radius, which requirement becomes more stringent with an approach of the measured section $x = X_a$ to the cavitator. For too small depth more narrow profile of the cavity forward part due to free boundary action as compared to infinite flow and small deformation of circular form of the cavity sections should be accounted additionally.

Conclusion

An essential refinement of the elementary equations of nearly axisymmetric cavities is performed. Based on this refinement, a procedure of accelerated estimate of experimental cavitation numbers and their adjustment for the respective supercavitating motion in the infinite flow is proposed and verified.

Acknowledgements

The author would like to thank Dr. Ronald Joslin, ONR for his support and encouragement.

References

[1] Guzevsky L. G. (1979). *Numerical analysis of cavitation flows*. [In Russian], Preprint No. 40-79 of CO AS USSR, Heat-Physics Institute, Novosibirsk,
[2] Logvinovich G.V. (1969). *Hydrodynamics of flows with free boundaries* [In Russian], Naukova Dumka, Kiev.
[3] Serebryakov V.V, Nechitailo N. (2015) *Hydrodynamics of supercavitating bodies at an angle of attack under conditions of considerable effect of fluid weightiness and closeness of free border*, J. JSOE, V. 5, pp. 255-265.
[4] Serebryakov V.V. (2009). *Physical-mathematical bases of the principle of independence of cavity expansion*/, Proc. CAV2009, paper No.169, Ann Arbor, Michigan, USA.
[5] Serebryakov V.V., Arndt R. E. A., Dzielski J. E. (2015). *Supercavitation: Theory, experiment and scale effects*, Proc. CAV2015, IOP: Conference series V. 656.